Supporting Information Corrected April 13, 2012

Supplementary Information:

A calcium-based plasticity model explains sensitivity of synaptic changes to spike pattern, rate and dendritic location

Michael Graupner[1,2,3]*and Nicolas Brunel[1,2]

[1] *Laboratoire de Neurophysique et Physiologie, Université Paris Descartes*

[2] *CNRS, UMR 8119;* [1,2] *45 rue des Saints Pères, 75270 Paris Cedex 06, France*

[3] *Center for Neural Science, New York University,*

4 Washington Place, New York, NY 10003-6603, USA

February 15, 2012

Contents

*Correspondence should be addressed to Michael Graupner, Center for Neural Science, New York University, 4 Washington Place, New York, NY 10003-6603, USA. michael.graupner@nyu.edu

1 Supplementary Figures

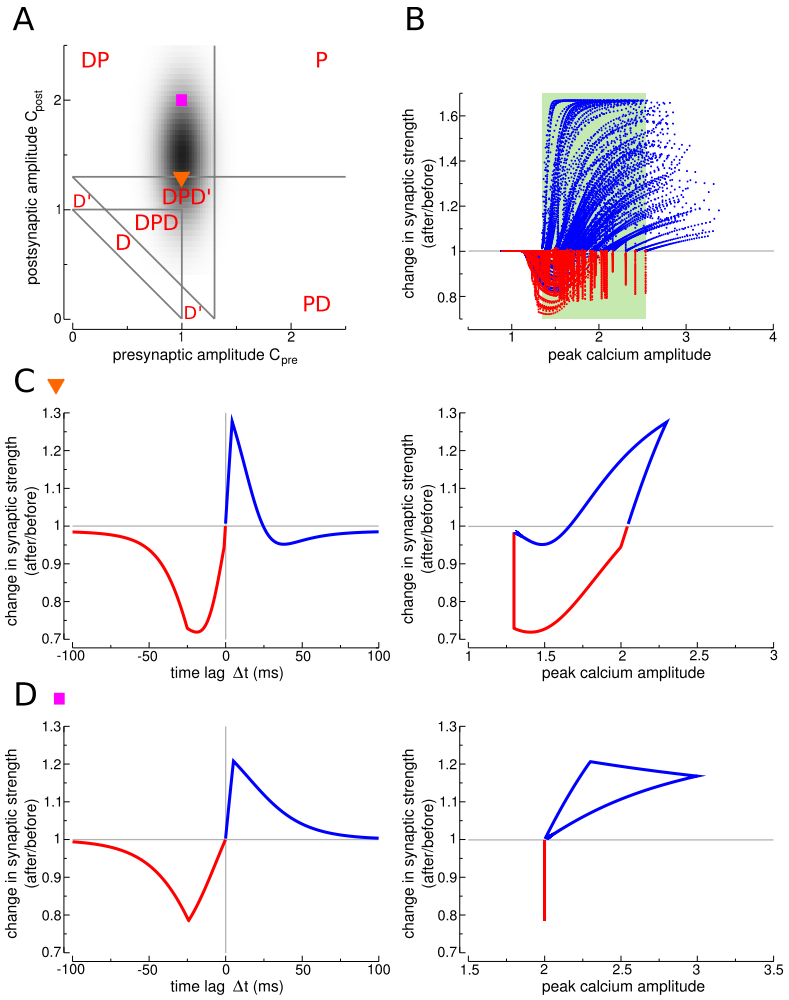

Figure S1: Direction of synaptic changes and maximal calcium amplitude. Which feature of the calcium transient predicts most reliably the direction and magnitude of synaptic changes? A long-standing hypothesis is that the maximal calcium amplitude induced by pre- and postsynaptic spikes is the key factor in determining the direction and magnitude of synaptic plasticity (Bear et al. 1987; Hansel et al. 1997; Yang et al. 1999; Cormier et al. 2001). Experimental data from Nevian and Sakmann (2006) show however that even though an elevation of calcium is necessary to induce synaptic changes, there is a large region of maximal calcium amplitudes for which both negative and positive weight changes are observed, depending on the order of pre- and postsynaptic activity (see Nevian and Sakmann 2006; Fig.8). We show here that our model naturally reproduces this phenomenon. (*A*) Location of the parameter sets in the $C_{\rm pre} - C_{\rm post}$ plane (orange triangle: $C_{\rm post} = 1.3$; magenta square: $C_{\rm post} = 2$; $C_{\rm pre} = 1$ in both cases; gray shaded region: bivariate Gaussian centered at $(\bar{C}_{\rm pre} = 1, \bar{C}_{\rm post} = 1.5)$, with standard deviations $(\sigma_{\rm pre} = 0.15, \sigma_{\rm post} = 0.4)$; see Tab. S3 for other parameters). (*B*) Change in synaptic strength as a function of the peak calcium amplitude for 100 sets of pre- and postsynaptic calcium amplitudes drawn randomly from the bivariate Gaussian distribution shown by the gray shaded region in *A*; γ_p is chosen in each case such that the amplitudes of LTP and LTD are approximately balanced. Three different regions appear: (i) low peak calcium amplitudes evoke LTD only, (ii) intermediate calcium amplitudes (green shaded region) induce both LTP and LTD, depending on the order of pre- and postsynaptic spikes, and (iii) high calcium amplitudes evoke LTP only. In region (ii), a given peak calcium amplitude can lead to bidirectional synaptic changes, as in experiments (Nevian and Sakmann 2006). Hence, the temporal dynamics of the calcium concentration is crucial to determine the direction and magnitude of plasticity outcomes. (*C,D*) Left panels: Changes in synaptic strength for two examples of $C_{\rm pre}$ and $C_{\rm post}$ (see symbols) as a function of Δt. Right panels: Changes in synaptic strength as a function of the maximal calcium amplitude of the compound calcium trace. Each point of the curves correspond to a different value of Δt. The red (blue) portion of the curves correspond to $\Delta t < 0$ ($\Delta t > 0$), respectively. All synaptic changes shown in this figure are in response to 60 spike-pair stimulations ($\Delta t \in [-100, 100]$) at 1 Hz.

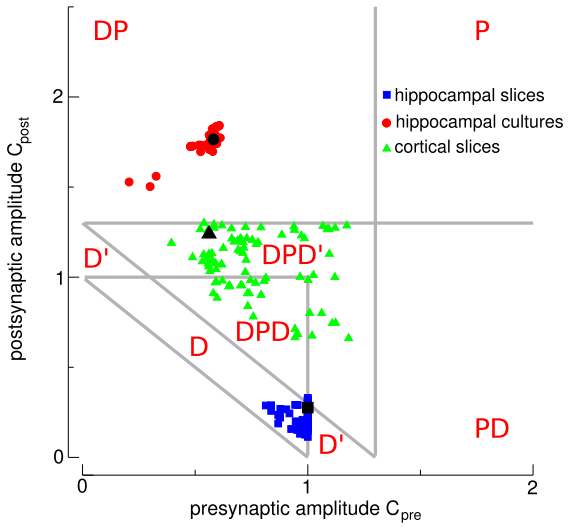

Figure S2: Plasticity results from different experiments are accounted for by distinct parameter sets. The C_{pre}-C_{post} plane is shown for $\theta_d = 1$, $\theta_p = 1.3$ as in Fig. 2*C*. The seven regions of different possible STDP outcomes for spike-pair stimulation are indicated by the potentiation (P) and depression (D) nomenclature (see Fig. 2). The blue, red and green symbols show outcomes from fitting our model to experimental data obtained in hippocampal slices (Wittenberg and Wang 2006), hippocampal cultures (Wang et al. 2005) and cortical slices (Sjöström et al. 2001), respectively. Fit results obtained from 100 randomly drawn initial conditions are shown for each of the four systems (SI Materials and Methods). The fit results used in Fig. 3, 4, 5, S3, S4, and S10 are shown as black symbols (see Tab. S2). Fits of the data from hippocampal slices lie in the D region, with small amplitudes of the pre-synaptically triggered calcium transient (Wang et al. 2005). Fits from hippocampal cultures lie in the DP region, with large amplitudes of the post-synaptically triggered calcium transient (Discussion) (Wang et al. 2005). Finally, fits of the data from cortical slices (Sjöström et al. 2001) lie in the DPD and DPD' region. Interestingly, all fits to the different data sets yield comparable presynaptic calcium amplitudes.

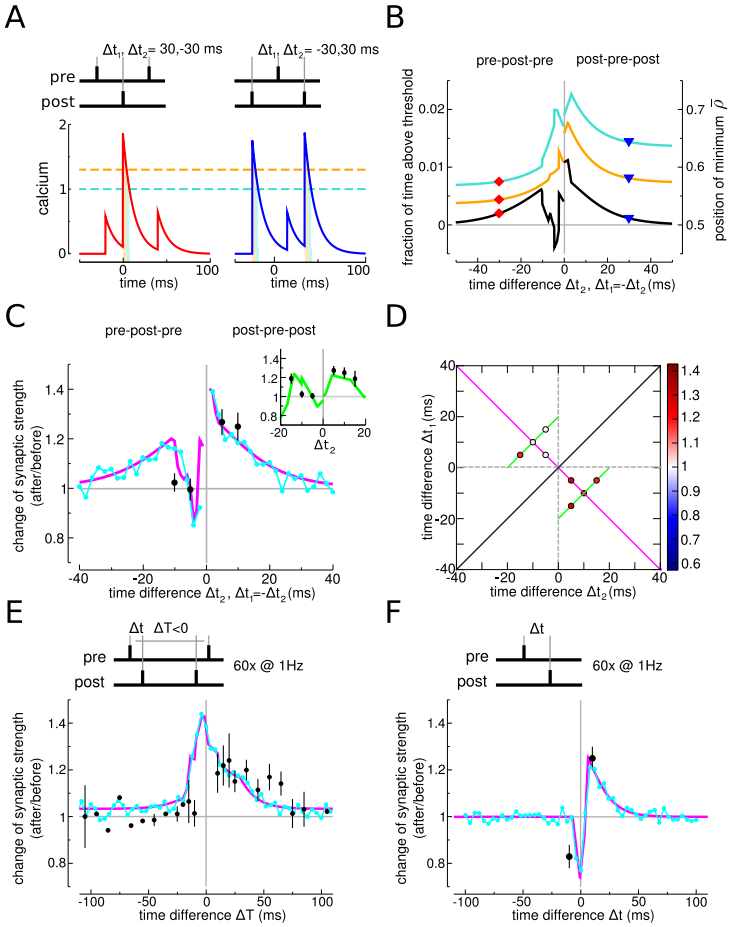

Figure S3: Nonlinearities in response to spike-triplet and -quadruplet stimulation in hippocampal cultures. (*A*) Calcium transients evoked by a pre-post-pre triplet (red line, $\Delta t_1 > 0$, $\Delta t_2 < 0$, see *SI Materials and Methods* for the convention of Δt_1 and Δt_2) and a post-pre-post triplet (blue, $\Delta t_1 < 0$, $\Delta t_2 > 0$). Note the large calcium transients evoked by postsynaptic spikes ($C_{\text{post}} = 1.7644$, $C_{\text{pre}} = 0.5816$). (*B*) The fractions of time spent above the depression (turquoise) and the potentiation threshold (orange, left-hand y-axis) as well as position of the potential minimum, $\bar{\rho}$, (black, right-hand y-axis) are shown with respect to Δt_2 for the case of symmetrical spike-triplets, *i.e.*, $\Delta t_1 = -\Delta t_2$. The two examples from *A* are indicated by symbols in the same color. (*C*) The change in synaptic strength for symmetrical spike-triplets ($\Delta t_1 = -\Delta t_2$) shows a clear imbalance, where pre-post-pre triplets evoke no change or little potentiation and post-pre-post triplets induce potentiation. The inset shows triplets with $\Delta t_1 = \Delta t_2 + 20$ ms for $-20 < \Delta t_2 < 0$ ms and $\Delta t_1 = \Delta t_2 - 20$ ms for $0 < \Delta t_2 < 20$ ms (see *D*). (*D*) The imbalance in plasticity outcomes between pre-post-pre and post-pre-post triplets becomes more apparent in the Δt_1 - Δt_2 plane. The color code depicts the change in synaptic strength as given by analytical results. Post-pre-post triplets evoke strong synaptic potentiation for small $|\Delta t_1|$ and $|\Delta t_2|$. The magenta and the green lines indicate the pairs of Δt_1, Δt_2 exemplified in *C* in the same color. The middle diagonal (black line) separates pre-post-pre and post-pre-post triplets. (*E*) In line with experiments, spike-quadruplet stimulation yields stronger potentiation for post-pre-pre-post quadruplets (convention: $\Delta T > 0$) as compared to pre-post-post-pre quadruplets ($\Delta T < 0$; $\Delta t = 5$ ms and -5 ms for pre-post and post-pre pairs, respectively). (*F*) Using the same parameter set as in *A*-*E*, the model reproduces the classical STDP curve (DP) in response to spike-pair stimulation as seen in experiments. All changes in synaptic strength are in response to the presentation of 60 motifs at 1 Hz. All data points in this figure are taken from Wang et al. (2005) (mean $\pm$ SEM, if multiple points are available). Analytical results of changes in synaptic strength are shown in magenta and simulation results in cyan. The 'hippocampal cultures' parameter set is used in this figure (see Tab. S2).

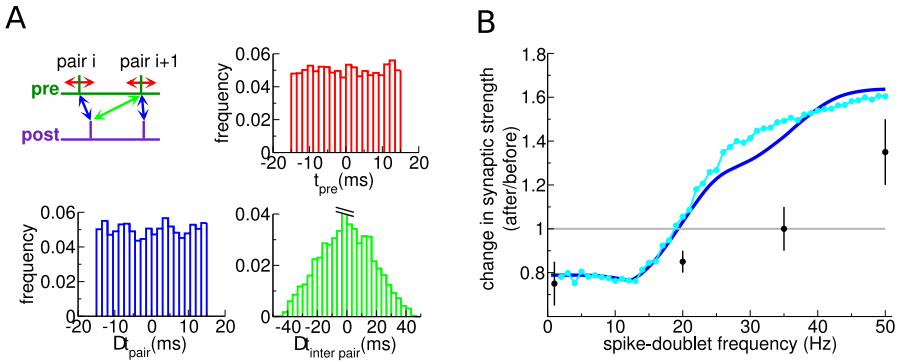

Figure S4: Synaptic changes for jittered spike-pairs. (*A*) In this stimulation protocol, the time of the the presynaptic spike, $t_{\rm pre}$, is drawn from a flat distribution of the interval $[-15, 15$ ms$]$ (red arrow), and the time difference within one spike-pair , $\Delta t_{\rm pair}$, is also drawn from a flat distribution of the interval $[-15, 15$ ms$]$ (blue arrows) (Sjöström et al. 2001). The distributions for $t_{\rm pre}$ and $\Delta t_{\rm pair}$ for 5000 spike-pairs are shown in red and blue, respectively. The distribution for pre-post ($\Delta t > 0$) or post-pre ($\Delta t < 0$) pairings with spikes from consecutive spike-pairs, $\Delta t_{\rm inter\,pair}$, is shown in green for a presentation frequency of $f = 50$ Hz (5000 spike-pairs). The peak at zero is discontinued and counts cases where a post-pre (pre-post) pair at time point i is followed by a pre-post pair (post-pre) at time point $i+1$, that is, two presynaptic (postsynaptic) spikes follow one another in consecutive spike-pairs. (*B*) Jittered spike-pairs evoke depression at low spike-pair presentation frequencies ($f < 19$ Hz) and potentiation at high frequencies ($f \geq 20$ Hz). Data points (black) are adapted from plasticity experiment in cortical slices (Sjöström et al. 2001) (mean $\pm$ SEM). Analytical results of change in synaptic strength are shown in blue and simulation results in cyan. Both are obtained using the 'cortical slices' parameter set (see Tab. S2). All transition probabilities are shown for the presentation of 75 spike-pairs.

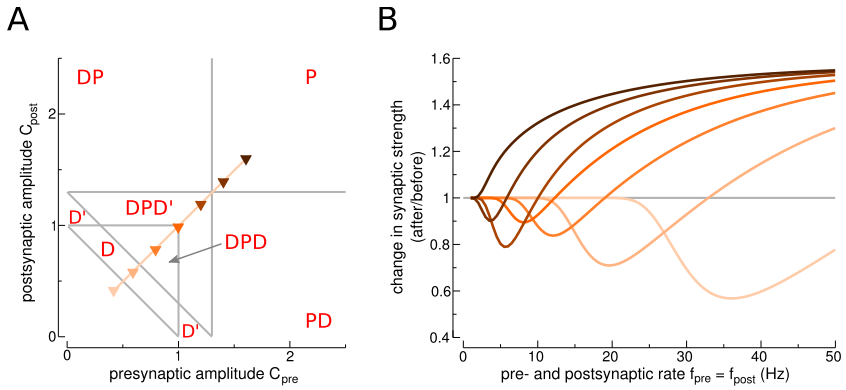

Figure S5: Activity-dependent calcium amplitudes lead to BCM rule (Bienenstock et al. 1982). (*A*) Values of $C_{\rm pre}$ and $C_{\rm post}$ used in *B* are indicated by triangles with various colors ($C_{\rm pre} = C_{\rm post} = 0.4, 0.6, 0.8, 1.0, 1.2, 1.4, 1.6$). All other parameters are kept constant (see Tab. S1). postsynaptic firing rates (for simplicity $f_{\rm pre} = f_{\rm post}$), for the values of pre- and postsynaptic calcium amplitudes indicated in *A* (same color code). For low calcium amplitudes, the synapse model exhibits only LTD in the physiological range of firing rates. Increasing the calcium amplitudes ($C_{\rm pre} = C_{\rm post}$) leads to the appearance of LTP at high frequencies, with a threshold between LTD and LTP that strongly depends on $C_{\rm pre} = C_{\rm post}$. Therefore, adding an activity dependence to the model, such that calcium amplitudes decrease when firing rates increase, would naturally leads to a BCM-like rule. A similar behavior can be obtained if potentiation and depression thresholds increase with firing rates.

2 Supplementary Tables

Parameter	unit	DP-curve	DPD-curve	DPD'-curve	P-curve	D -curve	D'-curve	BCM-example
τ_{Ca}	ms	20	20	20	20	20	20	20
C_{pre}		1	0.9	1	2	0.6	1	varied
C_{post}		2	0.9	2	2	0.6	2	varied
θ_d		1	1	1	1	1	1	1
θ_p		1.3	1.3	2.5	1.3	1.3	3.5	1.3
γ_d		200	250	50	160	500	60	200
γ_p		321.808	550	600	257.447	550	600	400
σ		2.8284	2.8284	2.8284	2.8284	5.6568	2.8284	2.8284
τ	s	150	150	150	150	150	150	150
$\rho_\star$		0.5	0.5	0.5	0.5	0.5	0.5	0.5
D	ms	13.7	4.6	2.2	0	0	0	0
β		0.5	0.5	0.5	0.5	0.5	0.5	0.5
b		5	5	5	5	5	5	5

Table S1: Parameters of the STDP curves depicted in Fig. 2*C,D* and the sliding threshold example in Fig. S5. The calcium amplitudes (C_{pre}, C_{post}) and the thresholds (θ_d, θ_p) define the locations in the θ_p-θ_d and the C_{pre}- C_{post} planes in Fig. 2*C,D*. The activation thresholds for all examples in the C_{pre}-C_{post} plane (DP, DPD, P and D, Fig. 2*C*) are $\theta_d = 1$ and $\theta_p = 1.3$. The calcium amplitudes for all examples in the θ_p-θ_d plane (DPD' and D', Fig. 2*D*) are $C_{\mathrm{pre}} = 1$ and $C_{\mathrm{post}} = 2$. γ_d, γ_p and σ are adjusted such that all examples yield approximately similar magnitudes of synaptic changes. The time delay of the presynaptic calcium transient, D, is adjusted such that the transition from depression to potentiation occurs at $\Delta t = 0$ ms for the DP, DPD and the DPD' examples, $D = 0$ otherwise. For simplicity, τ_{Ca}, τ, $\rho_\star$, β and b are kept the same for all examples.

Parameter	**hippocampal slices** (Wittenberg and Wang 2006) Fig. 3, S10	**hippocampal cultures** (Wang et al. 2005) Fig. S3, S10	**cortical slices** (Sjöström et al. 2001) Fig. 4, 5, S4
τ_{Ca} (ms)	48.8373	11.9536	22.6936
C_{pre}	1	0.58156	0.5617539
C_{post}	0.275865	1.76444	1.23964
θ_d	**1**	**1**	**1**
θ_p	**1.3**	**1.3**	**1.3**
γ_d	313.0965	61.141	331.909
γ_p	1645.59	113.6545	725.085
σ	9.1844	2.5654	3.3501
τ (sec)	688.355	33.7596	346.3615
$\rho_\star$	**0.5**	**0.5**	**0.5**
D (ms)	18.8008	10	4.6098
β	**0.7**	**0.5**	**0.5**
b	5.28145	36.0263	5.40988

Table S2: Parameters obtained from fitting the synapse model to experimental data. Values in bold were prefixed and were not allowed to be optimized by the fitting routine (SI Materials and Methods).

Parameter	unit	DPD'-curve (orange triangle)	DP-curve (magenta square)	heterogeneous curve (gray shaded area)
τ_{Ca}	ms	20	20	20
C_{pre}		1	1	drawn
C_{post}		1.3	2	drawn
θ_d		1	1	1
θ_p		1.3	1.3	1.3
γ_d		150	150	150
γ_p		310	241.356	adjusted
σ		2.8284	2.8284	2.8284
τ	s	150	150	150
$\rho_\star$		0.5	0.5	0.5
D	ms	4.3	13.8	adjusted
β		0.5	0.5	0.5
b		5	5	5

Table S3: Parameters of the examples for maximal calcium amplitude and direction of synaptic change depicted in Fig. S1. We vary C_{pre} and C_{post} to obtain qualitatively different STDP curves in the DPD' and the DP regions (Fig. S1*A*). γ_p and γ_d are adjusted to yield approximately equal LTP and LTD magnitudes across the different cases. D is chosen such that the transition from LTD to LTP occurs at $\Delta t = 0$ ms. For the examples illustrating synaptic heterogeneity (Fig. S1*B*), we draw the pre- and postsynaptic calcium amplitudes from a bivariate Gaussian distribution with means at $(\bar{C}_{\mathrm{pre}} = 1, \bar{C}_{\mathrm{post}} = 1.5)$ and standard deviations $(\sigma_{\mathrm{pre}} = 0.15, \sigma_{\mathrm{post}} = 0.4)$. All other parameters are kept constant across the cases.

Parameter	unit	min	max
τ_{Ca}	ms	1	100
C_{pre}		0.1	20
C_{post}		0.1	50
θ_d		**fixed**	
θ_p		**fixed**	
γ_d		5	5000
γ_p		5	2500
σ		0.35	70.7
τ	s	2.5	2500
$\rho_\star$		**fixed**	
D	ms	0	50
β		**fixed**	
b		1	100

Table S4: Parameter value ranges. When fitting the synapse model to the different experimental datasets ('hippocampal slices' Wittenberg and Wang 2006, 'hippocampal cultures' Wang et al. 2005, and 'cortical slices' Sjöström et al. 2001, we draw the initial parameter values from an uniform distribution within the boundaries given here. After convergence to a minima of the gradient descent routine (see SI Materials and Methods), we discard the fit result if the final parameter values lie outside those boundaries. We choose the boundaries to assure that the parameter values lie in biological plausible ranges.

3 Supplementary Materials and Methods

3.1 Calcium dynamics

We use two types of calcium models in this study. The simplified calcium model is used in the whole paper, except in Section 3.1.2, where we investigate the more realistic nonlinear calcium model.

3.1.1 Simplified calcium model

The postsynaptic calcium dynamics is described by

$$\frac{dc}{dt} = -\frac{c}{\tau_{\mathrm{Ca}}} + C_{\mathrm{pre}} \sum_i \delta(t - t_i - D) + C_{\mathrm{post}} \sum_j \delta(t - t_j), \tag{1}$$

where c is the total calcium concentration, τ_{Ca} the calcium decay time constant, and $C_{\mathrm{pre}}, C_{\mathrm{post}}$ the pre- and postsynaptically evoked calcium amplitudes. The sums go over all pre- and postsynaptic spikes occurring at times t_i and t_j, respectively. The time delay, D, between the presynaptic spike and the occurrence of the corresponding calcium transient (Fig. 1*A*) accounts for the slow rise time of the NMDAR-mediated calcium influx (see SI section 3.1.2 below). In practice, the delay is chosen such that the transition from LTD to LTP of the STDP curve occurs at $\Delta t = 0$ ms. This leads to delays in the range 0-25 ms. Without loss of generality, we set the resting calcium concentration to zero, *i.e.*, $c_0 = 0$, and use dimensionless calcium concentrations.

3.1.2 Nonlinear calcium model

We implement a more realistic calcium model (called in the following 'nonlinear' calcium model) to account for the following properties of postsynaptic calcium dynamics: (i) calcium transients mediated by NMDA receptors and VDCC have distinct dynamics. The NMDA mediated transient has a slow rise and decay time, while the VDCC mediates a fast calcium transient (Sabatini et al. 2002). (ii) Summation of pre and post transients is nonlinear when the post spike occurs after the pre spike. Preceding presynaptic activation paired with postsynaptic depolarization from the backpropagating action potential generates a large calcium influx through the NMDA receptor (see Fig. S6*A,C*, Nevian and Sakmann 2006).

In the nonlinear model, calcium transients evoked by pre- and postsynaptic spikes are accounted for by a difference of exponentials. Presynaptic calcium transients are described as

$$\frac{dA}{dt} = \tilde{A}\left(-\frac{A}{\tau^{\mathrm{r}}_{\mathrm{pre}}} + B\right) \tag{2}$$

$$\frac{dB}{dt} = -\frac{B}{\tau^{\mathrm{d}}_{\mathrm{pre}}} + \sum_i \delta(t - t_i), \tag{3}$$

where the sum goes over all presynaptic spikes occurring at times t_i. $\tau^{\mathrm{r}}_{\mathrm{pre}}$ and $\tau^{\mathrm{d}}_{\mathrm{pre}}$ are the rise and the decay time constants of the calcium transient, respectively, $\tau^{\mathrm{r}}_{\mathrm{pre}} = 10$ ms and $\tau^{\mathrm{d}}_{\mathrm{pre}} = 30$

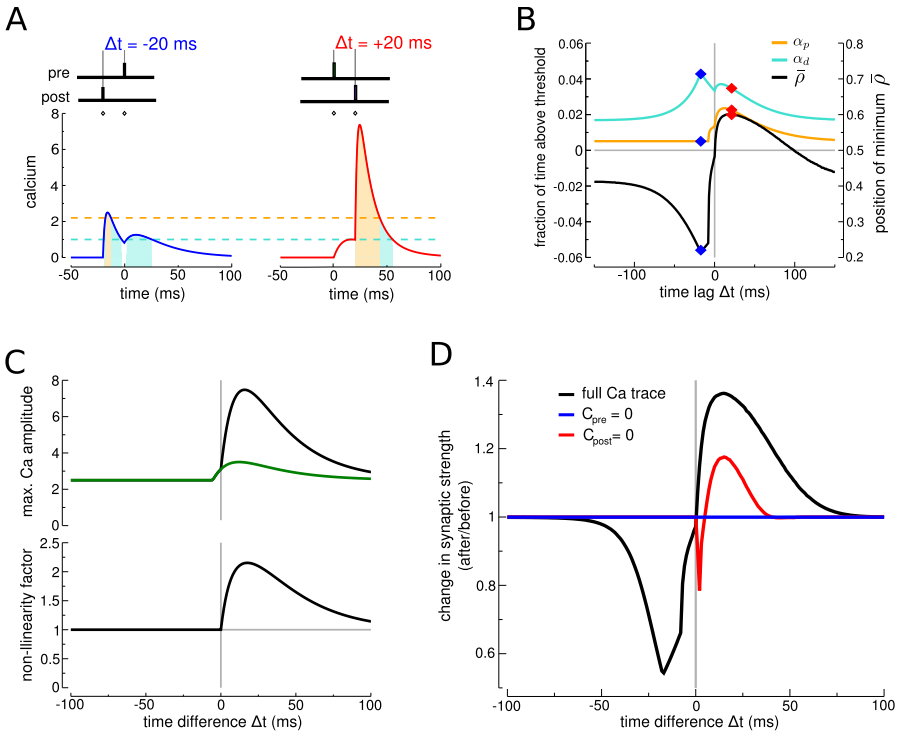

Figure S6: Synaptic changes induced by nonlinear and finite rise time calcium transients. (*A*) Calcium transients evoked by a post-pre (blue line) and a pre-post spike-pair (red line). Δt indicated in panel ($C_{\mathrm{pre}} = 1$, $C_{\mathrm{post}} = 2.5$. Note the nonlinear increase of the postsynaptically evoked calcium transient in case of a pre-post spike-pair. The large calcium influx stems from the voltage-dependence of the NMDA receptor (Nevian and Sakmann 2006, see SI Material and Methods for the 'nonlinear' calcium model). (*B*) Fraction of time spent above the depression (turquoise line) and potentiation thresholds (orange, left-hand y-axis), and the average asymptotic value of the synaptic efficacy ($\bar{\rho}$, black, right-hand y-axis) as a function of Δt. The two examples from *A* are indicated by diamonds. (*C*) Maximal amplitude and nonlinearity of the calcium transient. The upper panel compares the maximal amplitude of the full calcium trace (black line) with the maximal amplitude of the expected linear sum of pre- and postsynaptically evoked calcium transient (green line). The lower panel depicts the nonlinearity factor which is the peak calcium amplitude, normalized to the expected linear sum of pre- and postsynaptically evoked transients. A nonlinearity factor of one (gray line) indicates linear summation. (*D*) Change in synaptic strength generated by the nonlinear calcium model and with NMDA or VDCC blocked. The analytically calculated change in synaptic strength shows a DP behavior (black line). Blocking NMDA receptors (blue line, $C_{\mathrm{pre}} = 0$) abolishes plasticity, and blocking VDCC (red line, $C_{\mathrm{post}} = 0$) preserves LTP as seen in experiments (Bi and Poo 1998; Nevian and Sakmann 2006).

ms (Sabatini et al. 2002). $\tilde{A}$ is a scaling factor such that the maximal amplitude is given by $C_{\rm pre}$, $\tilde{A} = C_{\rm pre}\left((1/\tau^{\rm d}_{\rm pre} - 1/\tau^{\rm r}_{\rm pre})\left(\frac{\tau^{\rm r}_{\rm pre}}{\tau^{\rm d}_{\rm pre}}^{1/(1-\tau^{\rm r}_{\rm pre}/\tau^{\rm d}_{\rm pre})} - \frac{\tau^{\rm r}_{\rm pre}}{\tau^{\rm d}_{\rm pre}}^{1/(\tau^{\rm d}_{\rm pre}/\tau^{\rm r}_{\rm pre}-1)}\right)\right)^{-1}$.

Postsynaptic calcium transients are given by

$$\frac{dE}{dt} = \tilde{E}\left(-\frac{E}{\tau^{\rm r}_{\rm post}} + F\right) \quad (4)$$

$$\frac{dF}{dt} = -\frac{F}{\tau^{\rm d}_{\rm post}} + \sum_j \delta(t-t_j) + \eta \sum_j \delta(t-t_j)\cdot A, \quad (5)$$

where the sum goes over all postsynaptic spikes occurring at times t_j. $\tau^{\rm r}_{\rm post} = 2$ ms and $\tau^{\rm d}_{\rm post} = 12$ ms (Sabatini et al. 2002). η implements the increase of the NMDA mediated current in case of coincident presynaptic activation and postsynaptic depolarization through the backpropagating action potential. η determines by which amount the postsynaptically evoked calcium transient is increased in case of preceding presynaptic stimulation, in which case $A \neq 0$. $\tilde{D}$ is a scaling factor such that the maximal amplitude is given by $C_{\rm post}$, $\tilde{E} = C_{\rm post}\left((1/\tau^{\rm d}_{\rm post} - 1/\tau^{\rm r}_{\rm post})\left(\frac{\tau^{\rm r}_{\rm post}}{\tau^{\rm d}_{\rm post}}^{1/(1-\tau^{\rm r}_{\rm post}/\tau^{\rm d}_{\rm post})} - \frac{\tau^{\rm r}_{\rm post}}{\tau^{\rm d}_{\rm post}}^{1/(\tau^{\rm d}_{\rm post}/\tau^{\rm r}_{\rm post}-1)}\right)\right)^{-1}$.

The total calcium transient mediated by NMDA and VDCC activation is given by $c = A + D$. See Fig. S6*A* for two example calcium traces generated by the model described here. Using $\eta = 4$ yields a maximal nonlinearity factor of about 2 consistent with data from Nevian and Sakmann (2006) (Fig. S6*C*). Note that in contrast to the simplified calcium model, the presynaptically evoked calcium transient is *not* delayed in the nonlinear model.

We show in Fig. S6*D* that the nonlinear calcium model in combination with the synapse model described by Eq. [1] reproduce the 'classical' STDP curve, that is, depression for post-pre and potentiation for pre-post pairs. The conditions to observe a DP curve with the nonlinear calcium model are the same as in with the simplified calcium model, that is, the potentiation threshold is larger than the depression threshold ($\theta_p > \theta_d$), the amplitude of the postsynaptic calcium transient is larger than the potentiation threshold ($C_{\rm post} > \theta_p$), and the amplitude of the presynaptic transient is smaller than the potentiation threshold ($C_{\rm pre} < \theta_p$). Again, we impose that spike-pairs with large time differences do not evoke synaptic changes. This is the case if potentiation and depression evoked by a single postsynaptic spike cancel or nearly cancel each other (see Fig. S6*B,D* where $\bar{\rho}$ is not exactly 0.5 but no synaptic changes are induced since changes in ρ are small and not sufficient to build up). As with the simplified calcium model, these conditions yield the 'classical' STDP curve induced by nonlinear and finite rise time calcium transients in response to spike-pairs (Fig. S6*D*).

Note that the finite rise time of the NMDA mediated calcium transient moves the transition from LTD to LTP to $\Delta t \sim 0$ ms. In other words, the delay of the presynaptically evoked calcium transient introduced in the simplified calcium model can be seen as an effective implementation of the finite rise time of the NMDA-mediated calcium influx.

Importantly, the nonlinear synapse model reproduces the basic pharmacology of spike-pair evoked STDP. Blocking NMDA receptors, which is implemented by $C_{\rm pre} = 0$ in the model, abolishes LTD and LTP, as in experiments (Bi and Poo 1998; Nevian and Sakmann 2006). Note

that this NMDA dependence is also reproduced by the synapse model with simplified calcium dynamics, in large parameter regions (DP region where $C_{\rm pre} < \theta_d$). In addition, in the nonlinear model LTD is VDCC dependent, as in experiments (Bi and Poo 1998; Nevian and Sakmann 2006), whereas LTP is preserved for $C_{\rm post} = 0$ but with a smaller amplitude (Fig. S6*D*).

3.2 Analytical solution for transition probabilities

The behavior of the synapse model is governed by the fraction of time the calcium transient spends above the potentiation and the depression thresholds. In a given protocol, the average depression is given by γ_d times the fraction of time the calcium transient spends above θ_d, *i.e.* $\Gamma_d = \gamma_d \alpha_d$, and likewise for potentiation. The average fraction of time spent above a given threshold is

$$\alpha_x = \frac{1}{nT} \int_0^{nT} \Theta[c(t) - \theta_x] dt, \tag{6}$$

where nT refers to the duration of the stimulation protocol (n presentations at interval T; $x = p, d$). Analytical expressions for α_p and α_d for the stimulation protocols considered and the simplified calcium model can be found below. For pre- and postsynaptic Poisson firing, the amplitude distribution of the compound calcium trace can be calculated analytically (Gilbert and Pollak 1960), which in turn allows us to calculate α_p and α_d also for that case (see below).

To compute the transition probabilities, we perform a 'diffusion approximation' of ρ. We consider a periodic protocol, with a period $T \ll \tau$. During a period T, we assume that the calcium transient spends times of duration t_p/t_d above the potentiation/depression thresholds, respectively. Integrating Eq. (1) (in manuscript) over the interval $[t, t+T]$, and neglecting the cubic term, we have

$$\rho(t+T) \sim \rho(t) + \frac{t_p \gamma_p}{\tau}(1 - \rho(t)) - \frac{t_d \gamma_d}{\tau}\rho(t) + \sigma \sqrt{\frac{\tau_p + \tau_d}{\tau}} z(t),$$

where $z(t)$ is a Gaussian random variable of unit variance, or equivalently

$$\rho(t+T) \sim \rho(t) + \frac{T}{\tau}\left(\alpha_p \gamma_p (1 - \rho(t)) - \alpha_d \gamma_d \rho(t)\right) + \sigma \sqrt{\frac{T}{\tau}} \sqrt{\alpha_p + \alpha_d} z(t).$$

Hence, the conditional distribution Prob$(\rho(t+T)|\rho(t))$ is a Gaussian with a mean $\left(\alpha_p \gamma_p (1 - \rho(t)) - \alpha_d \gamma_d \rho(t)\right) T/\tau$ and a SD $\sigma \sqrt{\frac{T}{\tau}} \sqrt{\alpha_p + \alpha_d}$. This is the conditional distribution of the stochastic process given by

$$\tau \frac{d\rho}{dt} = \Gamma_p (1 - \rho) - \Gamma_d \rho - \rho(1 - \rho)(\rho_\star - \rho) + \sigma \sqrt{\tau} \sqrt{\alpha_p + \alpha_d} \eta(t). \tag{7}$$

Assuming γ_p and γ_d to be large allows us to neglect the cubic term, and turns equation (7) into an Ornstein-Uhlenbeck process. In that case, Eq. (7) can be solved analytically using the Fokker-Planck formalism (Risken 1996). The probability density function (pdf) of ρ is a time-dependent Gaussian,

$$P(\rho, t|\rho_0) = \frac{1}{\sqrt{\pi \sigma_\rho^2 \left(1 - e^{-2t/\tau_{\rm eff}}\right)}} \exp\left(- \frac{\left(\rho - \bar{\rho} + (\bar{\rho} - \rho_0) e^{-t/\tau_{\rm eff}}\right)^2}{\sigma_\rho^2 \left(1 - e^{-2t/\tau_{\rm eff}}\right)} \right), \tag{8}$$

where ρ_0 is the initial value of ρ at $t = 0$, which is 0 or 1 in this study depending on whether the system is initially in the DOWN or the UP state, respectively. $\bar{\rho}$ is the average value of ρ in the limit of a very long protocol equivalent to the minimum of the quadratic potential during the protocol, σ_ρ is the standard deviation of ρ in the same limit, and $\tau_{\rm eff}$ is the characteristic time scale of the temporal evolution of the pdf of ρ,

$$\bar{\rho} = \frac{\Gamma_p}{\Gamma_p + \Gamma_d}, \tag{9}$$

$$\sigma_\rho^2 = \frac{\sigma^2(\alpha_p + \alpha_d)}{\Gamma_p + \Gamma_d}, \tag{10}$$

$$\tau_{\rm eff} = \frac{\tau}{\Gamma_p + \Gamma_d}. \tag{11}$$

The integral of the pdf above or below the unstable fix-point, $\rho_\star$, at time nT, which marks the end of the stimulation protocol, gives the probability that the system will converge to the UP or the DOWN state. We denote the UP and the DOWN transition probabilities as $\mathcal{U}$ and $\mathcal{D}$, respectively. They are given by

$$\mathcal{U}(\rho_0) = \int_{\rho_\star}^{\infty} P(\rho, nT|\rho_0)d\rho \tag{12}$$

$$= \frac{1}{2}\left(1 + \text{erf}\left(-\frac{\rho_\star - \bar{\rho} + (\bar{\rho} - \rho_0)e^{-nT/\tau_{\rm eff}}}{\sqrt{\sigma_\rho^2\left(1 - e^{-2nT/\tau_{\rm eff}}\right)}}\right)\right), \tag{13}$$

as well as

$$\mathcal{D}(\rho_0) = \int_{-\infty}^{\rho_\star} P(\rho, nT|\rho_0)d\rho \tag{14}$$

$$= \frac{1}{2}\left(1 - \text{erf}\left(-\frac{\rho_\star - \bar{\rho} + (\bar{\rho} - \rho_0)e^{-nT/\tau_{\rm eff}}}{\sqrt{\sigma_\rho^2\left(1 - e^{-2nT/\tau_{\rm eff}}\right)}}\right)\right). \tag{15}$$

where erf refers to the standard Error Function, defined as $\text{erf}(x) = \frac{2}{\sqrt{\pi}}\int_0^x e^{-t^2}dt$.

3.3 No change in synaptic strength for spike-pairs with large time differences

Single pre- and postsynaptic spikes do not induce any synaptic changes in the model in two cases: (i) if they do not cross depression and potentiation thresholds (as for example in the DPD and PDP regions in Fig. 2*D*), (ii) or if contributions from depression and potentiation exactly cancel each other (as we impose in the DP and PD regions, for example). The latter is assured if the position of the quadratic potential during stimulation is at $\bar{\rho} = \rho_\star \equiv 0.5$, or in other words, if the temporal averages of the potentiation and the depression rates are equal: $\Gamma_p = \gamma_p\alpha_p = \Gamma_d = \gamma_d\alpha_d \Rightarrow \bar{\rho} = \Gamma_p/(\Gamma_p + \Gamma_d) = 0.5$. That requirement determines the ratio of the potentiation and the depression rate. Here, we demonstrate how to calculate that ratio

for one example where only single postsynaptic calcium transients cross both thresholds (that is $C_{\rm pre} < \theta_d < \theta_p < C_{\rm post}$) and give the ratios for all other cases. Note that the condition $\bar{\rho} = 0.5$ cannot be satisfied if one of the thresholds is never reached by single calcium transients (*e.g.*, D' in Fig. 2*C,D*).

A single post-synaptic spike induces a calcium transient described by $C_{\rm post} \exp(-t/\tau_{\rm Ca})$ in the simplified calcium model (see above). This transient crosses the depression threshold for a fraction of time $\alpha_d = \tau_{\rm Ca} \ln(C_{\rm post}/\theta_d)/T$, and the potentiation threshold for a shorter fraction of time $\alpha_p = \tau_{\rm Ca} \ln(C_{\rm post}/\theta_p)/T$, where T is the interval within which one spike-pair is presented. To ensure that single post-synaptic spikes do not induce any synaptic changes, we impose

$$\gamma_p \alpha_p = \gamma_d \alpha_d \;\Rightarrow\; \gamma_p \tau_{\rm Ca} \ln(C_{\rm post}/\theta_p)/T - \gamma_d \tau_{\rm Ca} \ln(C_{\rm post}/\theta_d)/T = 0, \tag{16}$$

which determines the ratio of potentiation and depression rate to

$$\gamma_p/\gamma_d = \frac{\ln(C_{\rm post}/\theta_d)}{\ln(C_{\rm post}/\theta_p)}. \tag{17}$$

That ratio of γ_p and γ_d ensures $\bar{\rho} = 0.5$ for large Δt in case $C_{\rm pre} < \theta_d < \theta_p < C_{\rm post}$.

The ratios of potentiation and depression rates for the other cases are given by

$$\gamma_p/\gamma_d = \begin{cases} \text{arbitrary} & C_{\rm pre}, C_{\rm post} < \theta_d, \theta_p, \\ \frac{\ln(C_{\rm post}/\theta_d)}{\ln(C_{\rm post}/\theta_p)} & C_{\rm pre} < \theta_d < \theta_p < C_{\rm post}, \\ \frac{\ln(C_{\rm post}/\theta_d)+\ln(C_{\rm pre}/\theta_d)}{\ln(C_{\rm post}/\theta_p)} & \theta_d < C_{\rm pre} < \theta_p < C_{\rm post}, \\ \frac{\ln(C_{\rm post}/\theta_d)+\ln(C_{\rm pre}/\theta_d)}{\ln(C_{\rm post}/\theta_p)+\ln(C_{\rm pre}/\theta_p)} & \theta_d < \theta_p < C_{\rm pre} < C_{\rm post}. \end{cases} \tag{18}$$

The ratios are given for the conditions $C_{\rm pre} < C_{\rm post}$ and $\theta_d < \theta_p$ but other cases can be derived in an equivalent way. Note that the ratios here are given for the simplified calcium model (see above).

3.4 Fraction of time spent above threshold for different stimulation protocols

We give here the analytical expressions for the fraction of time spent above threshold for the spike-pair, spike-triplet at low frequency, the spike-pair at varying frequencies and pre- and postsynaptic Poisson firing protocols. As an example, we focus on one particular case of calcium amplitudes and threshold, that is, $C_{\rm pre} < \theta < C_{\rm post}$. However, the expressions can be easily generalized to any relationship between calcium amplitudes and thresholds.

The fraction of time spent above threshold can be calculated analytically for the simplified calcium model. However, simple analytical expressions cannot be derived in the nonlinear model. All results presented in this section are derived for the simplified calcium model.

The fractions of time spent above threshold are used to calculate synaptic changes analytically in the model (see Methods section in manuscript). To simplify the expressions below, we rescale time with respect to the calcium time constant $\tau_{\rm Ca}$ as $t' \to t/\tau_{\rm Ca}$. Hence, both times and calcium amplitudes are dimensionless variables in what follows.

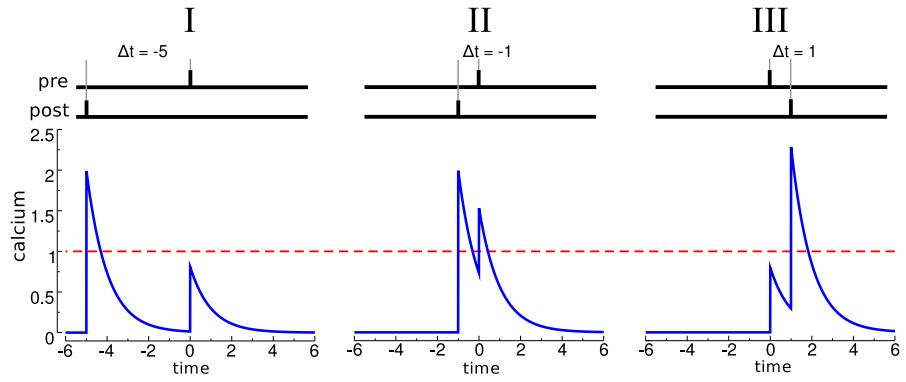

Figure S7: Single spike-pairs. Calcium transients for three different time differences, Δt, illustrate the three qualitatively different regions for calculating the fraction of time above threshold (see Eq. (21)). The parameters in the example are $C_{\rm pre} = 0.8$, $C_{\rm post} = 2$ and $\theta = 1$ (red dashed line).

Single spike-pairs We first consider a pair of one presynaptic spike at time $t = 0$ and one postsynaptic spike at time $t = \Delta t$. In the post-pre case ($\Delta t < 0$), the postsynaptic spike precedes the presynaptic spike and the calcium transient elicited by the spike-pair is given by

$$c(t) = \begin{cases} 0 & t < \Delta t, \\ C_{\rm post} \exp(\Delta t - t) & t \in [\Delta t, 0], \\ \exp(-t)\left(C_{\rm post} \exp(\Delta t) + C_{\rm pre}\right) & t > 0. \end{cases} \tag{19}$$

When $\Delta t > 0$, we have a pre-post pair, and

$$c(t) = \begin{cases} 0 & t < 0, \\ C_{\rm pre} \exp(-t) & t \in [0, \Delta t], \\ \exp(-t)\left(C_{\rm pre} \exp(\Delta t) + C_{\rm post}\right) & t > \Delta t. \end{cases} \tag{20}$$

Synaptic changes are potentially induced whenever $c(t)$ crosses the depression-, the potentiation-, or both thresholds. For $C_{\rm pre} < \theta < C_{\rm post}$, the fraction of time spent above a given threshold θ is separated into three qualitatively different intervals (Fig. S7) and given by

$$\alpha T = \begin{cases} \text{I} & \ln(C_{\rm post}/\theta) \\ & \quad \text{for } \Delta t < \ln((\theta - C_{\rm pre})/C_{\rm post}), \\ \text{II} & \ln(C_{\rm post}/\theta) + \ln((C_{\rm post} \exp(\Delta t) + C_{\rm pre})/\theta) \\ & \quad \text{for } \Delta t \in [\ln((\theta - C_{\rm pre})/C_{\rm post}), \ln(\theta/C_{\rm post})], \\ \text{III} & \ln(C_{\rm post}/\theta) + \ln((C_{\rm post} \exp(\Delta t) + C_{\rm pre})/(C_{\rm post} \exp(\Delta t))) \\ & \quad \text{for } \Delta t > \ln(\theta/C_{\rm post}). \end{cases} \tag{21}$$

T is the interval within which one spike-pair is presented.

Single spike-triplets The triplet cases investigated in that study involve either two presynaptic spikes paired with a postsynaptic one, or one presynaptic spike paired with two postsynaptic spikes. Note that the latter also accounts for the pre-spike with post-burst pairing as utilized

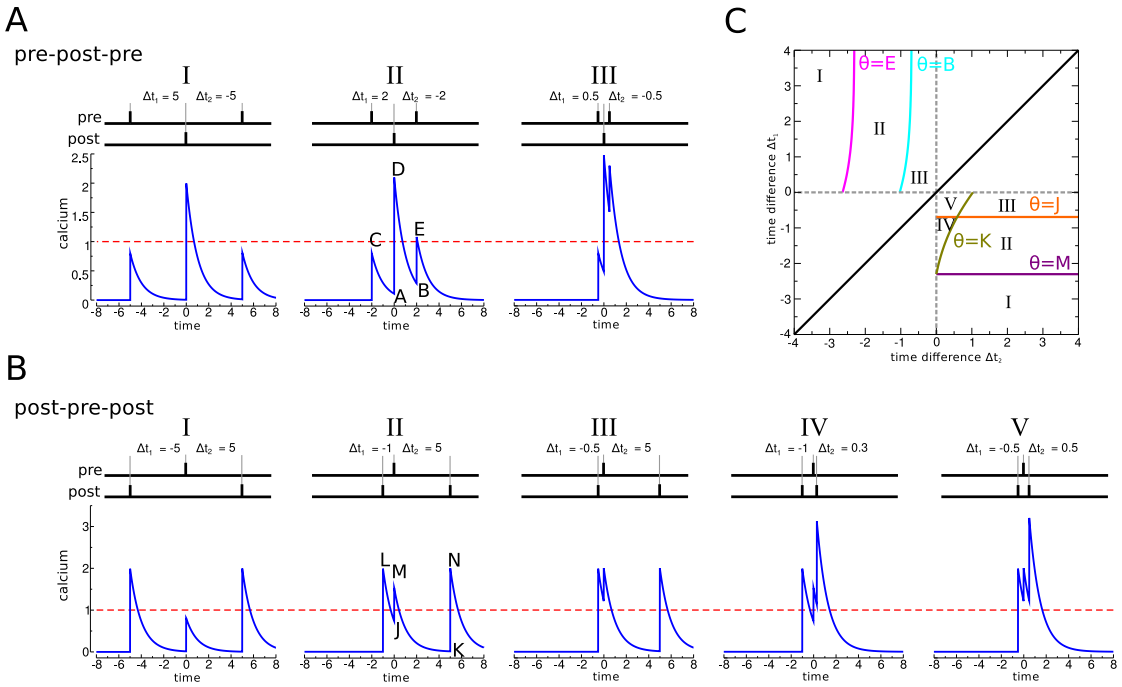

Figure S8: Single spike-triplets. (*A*) Pre-post-pre triplets yield three qualitatively different regions with respect to the calculation of the time spent above threshold (see Eq. (27)). The analytical expression for the points A-E are given in Eqs. (22)-(26). (*B*) Post-pre-post triplets yield five qualitatively different regions with respect to the calculation of the time spent above threshold (see Eq. (33)). The analytical expression for the points J-N are given in Eqs. (28)-(32). (*C*) The Δt_1-Δt_2 space is separated into six different regions with respect to the occurrence of pre- and postsynaptic spikes. The pre-post-pre quadrant (upper left) is furthermore divided into three different regions, I, II, and III, with respect to the calculation of α (illustrated in *A*). The post-pre-post quadrant (lower right) is divided into five different regions, I-V, with respect to the calculations of α (illustrated in *B*). The colored lines mark the points where the tops and foots of the calcium transients hit the threshold θ (as marked in panel). Those points mark the boundaries between the different regions for the calculation of α. The parameters in the given example are $C_{\mathrm{pre}} = 0.8$, $C_{\mathrm{post}} = 2$ and $\theta = 1$ (red dashed lines).

in Wittenberg and Wang (2006). In triplets, the single spike is used as a reference and Δt_1 is the time difference to the first other spike and Δt_2 the time difference to the second other spike with respect to the reference spike. Spike-triplets can be separated into six different regions with respect to the temporal order of spikes: (i) pre-pre-post, (ii) pre-post-pre, (iii) post-pre-pre, (iv) post-post-pre, (v) post-pre-post, and (vi) pre-post-post, where the former three are triplets with two presynaptic- and one postsynaptic spike and vice versa for the latter three (Fig. S3*D*). See Fig. S3*D* for the convention of the sign for Δt_1 and Δt_2 with respect to the spike order. Here, we illustrate the calculation of the fraction of time spent above threshold for the pre-post-pre and the post-pre-post examples, the other spike-triplet cases and the α's for spike-quadruplets can be calculated accordingly.

For pre-post-pre triplets, let us call A/B the values of the calcium amplitude at the foot of the second and the third transient, and C/D/E the values of the calcium amplitude at the top of the first, the second and the third transient (Fig. S8*A*). Those values are given by

$$\begin{aligned} A &= C_{\mathrm{pre}} \exp(-|\Delta t_1|)), && (22)\\ B &= C_{\mathrm{pre}} \exp(-(|\Delta t_1| + |\Delta t_2|)) + C_{\mathrm{post}} \exp(-|\Delta t_2|), && (23)\\ C &= C_{\mathrm{pre}}, && (24)\\ D &= A + C_{\mathrm{post}}, && (25)\\ E &= B + C_{\mathrm{pre}}. && (26) \end{aligned}$$

For $C_{\mathrm{pre}} < \theta < C_{\mathrm{post}}$, the fraction of time spent above a given threshold θ is separated into three qualitatively different intervals (Fig. S8*A,C*) and given by

$$\alpha T = \begin{cases} \mathrm{I} & \ln(D/\theta) \\ & \quad \text{for } |\Delta t_2| > \ln\left(\frac{C_{\mathrm{post}}+C_{\mathrm{pre}}\exp(-|\Delta t_1|)}{\theta - C_{\mathrm{pre}}}\right), \\ \mathrm{II} & \ln(D/\theta) + \ln(E/\theta) \\ & \quad \text{for } |\Delta t_2| \in [\ln\left(\frac{C_{\mathrm{post}}+C_{\mathrm{pre}}\exp(-|\Delta t_1|)}{\theta}\right), \ln\left(\frac{C_{\mathrm{post}}+C_{\mathrm{pre}}\exp(-|\Delta t_1|)}{\theta - C_{\mathrm{pre}}}\right)], \\ \mathrm{III} & \ln(E/\theta) + |\Delta t_2| \\ & \quad \text{for } |\Delta t_2| \leq \ln\left(\frac{C_{\mathrm{post}}+C_{\mathrm{pre}}\exp(-|\Delta t_1|)}{\theta}\right). \end{cases} \quad (27)$$

For post-pre-post triplets, let us call J/K the values of the calcium amplitude at the foot of the second and the third transient, and L/M/N the values of the calcium amplitude at the top of the first, the second and the third transient (Fig. S8*B*). Those values are given by

$$\begin{aligned} J &= C_{\mathrm{post}} \exp(-|\Delta t_1|)), && (28)\\ K &= C_{\mathrm{post}} \exp(-(|\Delta t_1| + |\Delta t_2|)) + C_{\mathrm{pre}} \exp(-|\Delta t_2|), && (29)\\ L &= C_{\mathrm{post}}, && (30)\\ M &= J + C_{\mathrm{pre}}, && (31)\\ N &= K + C_{\mathrm{post}}. && (32) \end{aligned}$$

For $C_{\mathrm{pre}} < \theta < C_{\mathrm{post}}$, the fraction of time spent above a given threshold θ is separated into five

qualitatively different intervals (Fig. S8*B,C*) and given by

$$\alpha T = \begin{cases} \text{I} & \ln(L/\theta) + \ln(N/\theta) \\ & \quad \text{for } |\Delta t_1| > \ln\left(\frac{C_{\rm post}}{\theta - C_{\rm pre}}\right), \\ \text{II} & \ln(L/\theta) + \ln(M/\theta) + \ln(N/\theta) \\ & \quad \text{for } |\Delta t_1| \in [\ln\left(\frac{C_{\rm post}}{\theta}\right), \ln\left(\frac{C_{\rm post}}{\theta - C_{\rm pre}}\right)] \\ & \quad \text{and } |\Delta t_2| > \ln\left(\frac{C_{\rm post}\exp(-|\Delta t_1|) + C_{\rm pre}}{\theta}\right), \\ \text{III} & \ln(M/\theta) + |\Delta t_1| + \ln(N/\theta) \\ & \quad \text{for } |\Delta t_1| \leq \ln\left(\frac{C_{\rm post}}{\theta}\right) \\ & \quad \text{and } |\Delta t_2| > \ln\left(\frac{C_{\rm post}\exp(-|\Delta t_1|) + C_{\rm pre}}{\theta}\right), \\ \text{IV} & \ln(L/\theta) + \ln(N/\theta) + |\Delta t_2| \\ & \quad \text{for } |\Delta t_1| > \ln\left(\frac{C_{\rm post}}{\theta}\right) \\ & \quad \text{and } |\Delta t_2| \leq \ln\left(\frac{C_{\rm post}\exp(-|\Delta t_1|) + C_{\rm pre}}{\theta}\right), \\ \text{V} & \ln(N/\theta) + |\Delta t_1| + |\Delta t_2| \\ & \quad \text{for } |\Delta t_1| \leq \ln\left(\frac{C_{\rm post}}{\theta}\right) \\ & \quad \text{and } |\Delta t_2| \leq \ln\left(\frac{C_{\rm post}\exp(-|\Delta t_1|) + C_{\rm pre}}{\theta}\right). \end{cases} \tag{33}$$

T is the interval within which one spike-triplet is presented.

Spike-pairs at frequency f We now consider the case where spike-pairs are repeatedly presented at a given frequency f (Sjöström et al. 2001). In contrast to single spike-pairs, calcium transients from successive spike pairs start to interact with each other at sufficiently high frequencies. Note that the time difference should always be smaller than the interval within which one spike pair is presented, *i.e.*, $\Delta t < T = 1/f$.

Here, we separately consider the post-pre and pre-post cases, that is, $\Delta t < 0$ and $\Delta t > 0$. For post-pre pairs, let us call B/C the values of the calcium amplitude at the foot of the post/pre-synaptic transient, and D/E the values of the calcium amplitude at the top of the post/pre-synaptic transient (Fig. S9*A*). We have, for $\Delta t < 0$,

$$B = (A(f) - 1)(C_{\rm post} + C_{\rm pre}\exp(-\Delta t)), \tag{34}$$
$$C = C_{\rm post}A(f)\exp(\Delta t) + (A(f) - 1)C_{\rm pre}, \tag{35}$$
$$D = A(f)C_{\rm post} + (A(f) - 1)C_{\rm pre}\exp(-\Delta t), \tag{36}$$
$$E = A(f)(C_{\rm post}\exp(\Delta t) + C_{\rm pre}), \tag{37}$$

where

$$A(f) = \frac{1}{1 - \exp(-1/f)}, \tag{38}$$

represents the peak calcium concentration, which increases with f due to summation of calcium transients induced by successive spike-pairs.

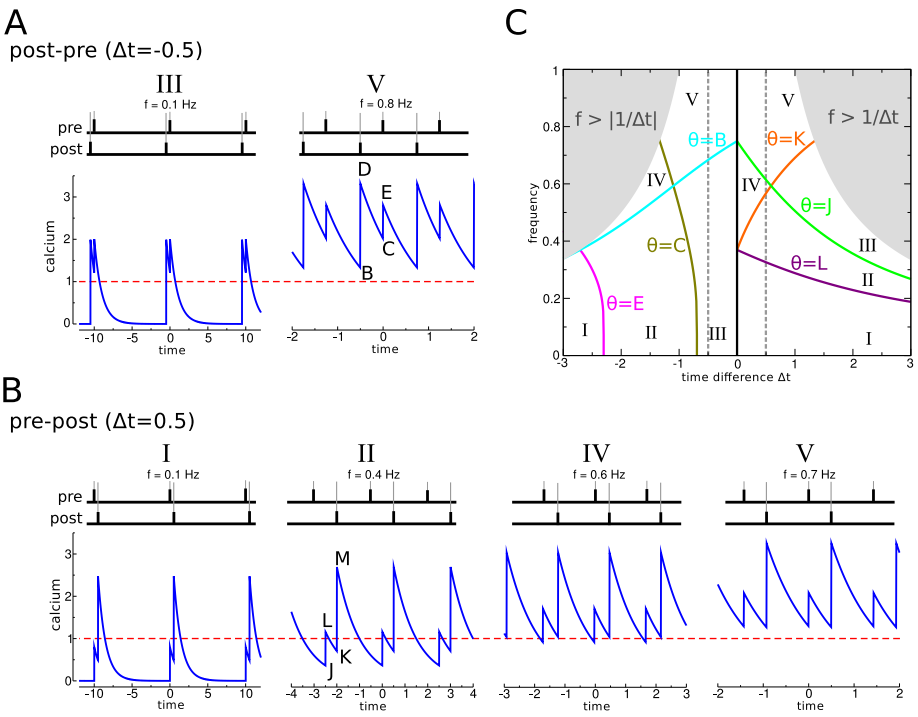

Figure S9: Spike-pairs vs frequency f. (*A*) There are in total five different regions with respect to the calculation of the fraction of time spent above threshold for post-pre pairs and varying presentation frequencies f (see also *C* and Eqs. (39)). For $\Delta t = -0.5$, the two different cases are illustrated. The analytical expressions for B-E are given in Eqs. (34)-(37). (*B*) Again, there exist in total five different regions with respect to the calculation of the fraction of time spent above threshold for pre-post pairs vs f (see also *C* and Eqs. (44)). Spike-pairs with $\Delta t = 0.5$ cover four of them which are illustrated here. The analytical expressions for J-M are given in Eqs. (40)-(43). (*C*) The f-Δt space is divided in post-pre ($\Delta t < 0$) and pre-post ($\Delta t > 0$) regions, which are each further subdivided into five qualitatively different regions with respect to the calculation of α (Eqs. (39) and (44)). The colored lines mark the points where the tops and foots of the calcium transients hit the threshold θ (as marked in panel). Those points mark the boundaries between the five different regions for post-pre- and pre-post pairs. The space is restricted by the fact that Δt should be smaller than one presentation cycle, that is, $|\Delta t| < 1/f$ (gray shaded regions). The gray dashed lines mark the examples $\Delta t = -0.5$ and 0.5 from *A* and *B*, respectively. The parameters in the given example are $C_{\mathrm{pre}} = 0.8$, $C_{\mathrm{post}} = 2$ and $\theta = 1$ (red dashed line).

For post-pre pairs and $C_{\rm pre} < \theta < C_{\rm post}$, the fraction of time spent above a given threshold θ is separated into five qualitatively different intervals (Fig. S9*C*) and given by

$$\alpha T = \begin{cases} \text{I} & \ln(D/\theta) \\ & \text{for } f < -\ln(1-(C_{\rm post}\exp(\Delta t)+C_{\rm pre})/\theta)^{-1}, \\ \text{II} & \ln(D/\theta)+\ln(E/\theta) \\ & \text{for } f \in [-\ln(1-(C_{\rm post}\exp(\Delta t)+C_{\rm pre})/(\theta+C_{\rm pre}))^{-1}, -\ln(1-(C_{\rm post}\exp(\Delta t)+C_{\rm pre})/\theta)^{-1}] \\ & \text{and } f < -\ln(1-(C_{\rm post}+C_{\rm pre}\exp(-\Delta t))/(\theta+C_{\rm post}+C_{\rm pre}\exp(-\Delta t)))^{-1}, \\ \text{III} & \ln(E/\theta)+|\Delta t| \\ & \text{for } f > -\ln(1-(C_{\rm post}\exp(\Delta t)+C_{\rm pre})/(\theta+C_{\rm pre}))^{-1} \\ & \text{and } f < -\ln(1-(C_{\rm post}+C_{\rm pre}\exp(-\Delta t))/(\theta+C_{\rm post}+C_{\rm pre}\exp(-\Delta t)))^{-1}, \\ \text{IV} & \ln(D/\theta)+1/f-|\Delta t| \\ & \text{for } f \in [-\ln(1-(C_{\rm post}\exp(\Delta t)+C_{\rm pre})/(\theta+C_{\rm pre}))^{-1}, -\ln(1-(C_{\rm post}\exp(\Delta t)+C_{\rm pre})/\theta)^{-1}] \\ & \text{and } f > -\ln(1-(C_{\rm post}+C_{\rm pre}\exp(-\Delta t))/(\theta+C_{\rm post}+C_{\rm pre}\exp(-\Delta t)))^{-1}, \\ \text{V} & 1/f \\ & \text{for } f > -\ln(1-(C_{\rm post}\exp(\Delta t)+C_{\rm pre})/(\theta+C_{\rm pre}))^{-1} \\ & \text{and } f > -\ln(1-(C_{\rm post}+C_{\rm pre}\exp(-\Delta t))/(\theta+C_{\rm post}+C_{\rm pre}\exp(-\Delta t)))^{-1}. \end{cases} \tag{39}$$

For pre-post pairs, let us call J/K the values of the calcium amplitude at the foot of the pre/post-synaptic transient, and L/M the values of the calcium amplitude at the top of the pre/post-synaptic transient (Fig. S9*B*). We have, for $\Delta t > 0$,

$$J = (A(f)-1)(C_{\rm post}\exp(\Delta t)+C_{\rm pre}), \tag{40}$$

$$K = (A(f)-1)C_{\rm post}+A(f)C_{\rm pre}\exp(-\Delta t)), \tag{41}$$

$$L = (A(f)-1)C_{\rm post}\exp(\Delta t)+A(f)C_{\rm pre}, \tag{42}$$

$$M = A(f)(C_{\rm post}+C_{\rm pre}\exp(-\Delta t)). \tag{43}$$

For pre-post pairs and $C_{\rm pre} < \theta < C_{\rm post}$, the fraction of time spent above a given threshold θ is also separated into five qualitatively different intervals (Fig. S9*C*) and given by

$$\alpha T = \begin{cases} \text{I} & \ln(M/\theta) \\ & \text{for } f < -\ln(1-(C_{\rm post}\exp(\Delta t)+C_{\rm pre})/(\theta+C_{\rm post}\exp(\Delta t)))^{-1}, \\ \text{II} & \ln(L/\theta)+\ln(M/\theta) \\ & \text{for } f \in [-\ln(1-(C_{\rm post}\exp(\Delta t)+C_{\rm pre})/(\theta+C_{\rm post}\exp(\Delta t)))^{-1} \\ & \qquad -\ln(1-(C_{\rm post}+C_{\rm pre}\exp(-\Delta t))/(\theta+C_{\rm post}))^{-1}] \\ & \text{and } f < -\ln(1-(C_{\rm post}\exp(\Delta t)+C_{\rm pre})/(\theta+C_{\rm post}\exp(\Delta t)+C_{\rm pre}))^{-1}, \\ \text{III} & \ln(M/\theta)+|\Delta t| \\ & \text{for } f > -\ln(1-(C_{\rm post}+C_{\rm pre}\exp(-\Delta t))/(\theta+C_{\rm post}))^{-1}] \\ & \text{and } f < -\ln(1-(C_{\rm post}\exp(\Delta t)+C_{\rm pre})/(\theta+C_{\rm post}\exp(\Delta t)+C_{\rm pre}))^{-1}, \\ \text{IV} & \ln(L/\theta)+1/f-|\Delta t| \\ & \text{for } f \in [-\ln(1-(C_{\rm post}\exp(\Delta t)+C_{\rm pre})/(\theta+C_{\rm post}\exp(\Delta t)))^{-1} \\ & \qquad -\ln(1-(C_{\rm post}+C_{\rm pre}\exp(-\Delta t))/(\theta+C_{\rm post}))^{-1}] \\ & \text{and } f > -\ln(1-(C_{\rm post}\exp(\Delta t)+C_{\rm pre})/(\theta+C_{\rm post}\exp(\Delta t)+C_{\rm pre}))^{-1}, \\ \text{V} & 1/f \\ & \text{for } f > -\ln(1-(C_{\rm post}+C_{\rm pre}\exp(-\Delta t))/(\theta+C_{\rm post}))^{-1}] \\ & \text{and } f > -\ln(1-(C_{\rm post}\exp(\Delta t)+C_{\rm pre})/(\theta+C_{\rm post}\exp(\Delta t)+C_{\rm pre}))^{-1}. \end{cases} \tag{44}$$

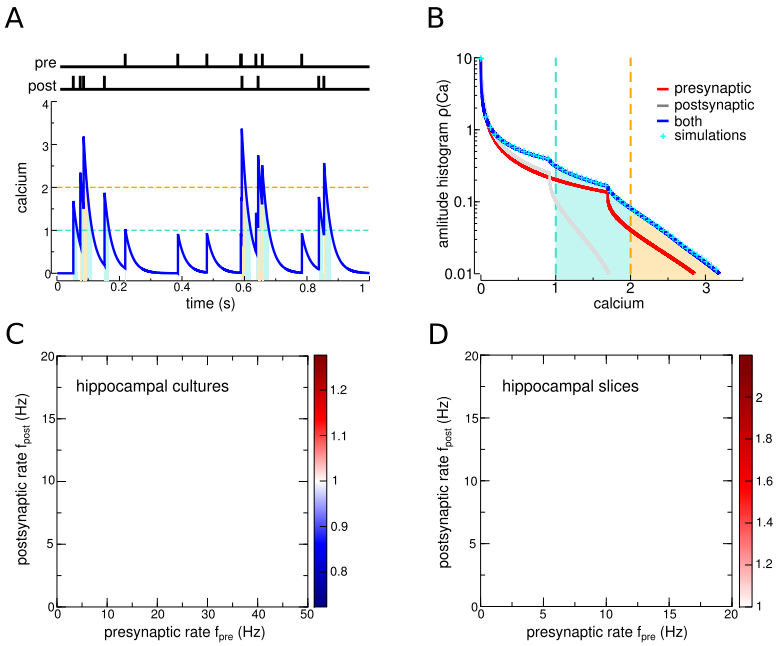

Figure S10: Dependence of plasticity on pre- and postsynaptic firing rates when both neurons fire as Poisson processes. (*A*) Example of a compound calcium transient (1 sec) evoked by pre- and postsynaptic Poisson firing at 10 Hz. (*B*) The individual pre- (red) and postsynaptically (gray) evoked distributions of calcium amplitudes resulting from Poisson firing at 10 Hz fall off sharply beyond the pre- and the postsynaptically evoked calcium amplitudes $C_{\mathrm{pre}} = 0.921$ and $C_{\mathrm{post}} = 1.693$, respectively. The amplitude distribution of the compound calcium trace (blue) is the convolution of the individual amplitude distributions (analytical result in blue and simulation results in cyan). (*C,D*) The change in synaptic strength (analytical results) in response to Poisson stimulation is shown for all combinations of pre- and postsynaptic rates for the 'hippocampal cultures' (*C*) and the 'hippocampal slices' (*D*) parameter sets (see Tab. S2). All results are induced by a stimulation lasting 10 sec.

$T = 1/f$ is the interval within which one spike-triplet is presented.

3.5 Pre- and postsynaptic Poisson firing

Most stimulation protocols utilize deterministic spike trains. These firing patterns are at odds with experimentally recorded spike trains *in vivo*, which show a pronounced temporal variability, similar to a Poisson process. We therefore investigated the behavior of the model in response to uncorrelated Poisson spike trains of pre- and postsynaptic neurons (Fig. S10*A*).

The amplitude distribution of a shot noise process, that is, a superposition of impulses occurring at random Poisson distributed times, can be calculated analytically for various shapes, $F(t)$, of the impulses (Gilbert and Pollak 1960). In the simplified calcium model, the shape function takes the form $F(t) = \exp(-t)$ (with normalized amplitude and rescaled time constant). We illustrate here shortly how to calculate the amplitude distribution for a single Poisson process (*e.g.*, pre- or presynaptic).

For a single Poisson process, the calcium amplitude density function, $P(c)$ is given in the

interval $0 \leq c < 1$ by

$$P(c) = \kappa c^{f-1}. \tag{45}$$

where f is the frequency of the Poisson process and κ is given by

$$\kappa = \frac{\exp(-f\gamma)}{\Gamma(f)}, \tag{46}$$

where $\gamma = 0.57721...$ is Euler's constant and $\Gamma(f)$ the Gamma function.

The amplitude density function is given by an integral form for calcium amplitudes $1 \leq c$

$$P(c) = c^{f-1}\left[\kappa - f\int_1^c P(x-1)x^{-f}dx\right]. \tag{47}$$

Note that this equation has to be solved iteratively. That means that we can determine $P(c)$ for $n \leq c < n+1$ from the knowledge of $P(c)$ for $n-1 \leq c < n$ (see Gilbert and Pollak 1960 for more details).

The amplitude distribution induced by independent pre- and postsynaptic firing at rates f_{pre} and f_{post} and with calcium amplitudes C_{pre} and C_{post} is simply the convolution of the individual amplitude distributions (Gilbert and Pollak 1960) (see Fig. S10*B*). In turn, the integral of the compound amplitude distribution above θ_d and θ_p yields α_d and α_p, respectively, and in turn the changes in synaptic strength as a function of pre- and postsynaptic firing rates f_{pre} and f_{post}. As in the case of deterministic protocols, we find that many qualitatively distinct types of behaviors can be obtained, depending on parameters. In Fig. 4*C,D* and Fig. S10, we focus on the three types of behaviors produced by the parameter sets that fit the three experiments described in the main text: 'hippocampal cultures' (Wang et al. 2005), 'hippocampal slices' (Wittenberg and Wang 2006), and 'cortical slices' (Sjöström et al. 2001).

The synapse model predicts that pre-and postsynaptic firing contribute in a similar way to synaptic efficacy changes in the cortex: No change for low pre and post rates, LTD for intermediate rates, and LTP for high rates (Fig. 4*C,D*). Due to the amplitude difference ($C_{\mathrm{post}} > C_{\mathrm{pre}}$), this behavior emerges at lower postsynaptic rates compared to presynaptic rates. In contrast, parameters fitting the hippocampal culture experiments lead to a completely different prediction for the dependence on pre and post firing. LTD is obtained for high presynaptic firing and low postsynaptic firing rates, whereas LTP occurs for large postsynaptic firing rates (Fig. S10*C*). This is again due to the imbalance between the amplitudes of the pre-and post-synaptically triggered calcium transients. Finally, parameters fitting the hippocampal slice experiments lead to qualitatively similar results as the visual cortex experiments at large pre and/or post rates, but yield no changes at low pre-post rates (Fig. S10*D*). This is due to the fact that the potentiation rate is much larger in hippocampal slices (see Tab. S2).

3.6 Synaptic Strength, Change in Synaptic Strength, and Simulations

We assume the synaptic strength is linearly related to ρ as $w = w_0 + \rho(w_1 - w_0)$, where w_0/w_1 is the synaptic strength of the DOWN/UP state. Synaptic strength as used here is typically measured in experiments as the excitatory postsynaptic potential (EPSP)/excitatory postsynaptic current (EPSC) amplitude, the initial EPSP slope, or the current in a 2-ms window at the peak of

the EPSC. We assume that, before a stimulation protocol, a fraction β of the synapses is in the DOWN state. The average initial synaptic strength is, therefore, equal to $\beta w_0 + [1-\beta]w_1$. After the stimulation protocol, the average synaptic strength is $w_0[(1-\mathcal{U})\beta + \mathcal{D}(1-\beta)] + w_1[\mathcal{U}\beta + (1-\mathcal{D})(1-\beta)]$. As in experiments, we consider the change in synaptic strength as the ratio between the average synaptic strengths after and before the stimulation (i.e., $[(1-\mathcal{U})\beta + \mathcal{D}(1-\beta)] + (b[\mathcal{U}\beta + (1-\mathcal{D})(1-\beta)])/(\beta + [1-\beta]b)$, where $b = w_1/w_0$). The average changes in synaptic strength were obtained by repeating simulations of the full model (Eq. 1) 1,000 times with identical model parameters but different random number generator seeds for the Gaussian white noise process.

3.7 Fitting the synapse model to experimental data, parameter choices

To fit hippocampal slice data (Wittenberg and Wang 2006), we include all three datasets into the cost function to be minimized (Fig. 3B, D, and E). To fit hippocampal culture results (Wang et al. 2005), we used the spike triplet as well as the quadruplet datasets to fit the parameters (Fig. S3C and E) and predict the spike pair data (Fig. S3F). To fit cortical slice results (Sjöström et al. 2001), only the data for regular spike pair presentations are taken into account (Fig. 4A). Here, jittered spike pair stimulations are qualitatively accounted for by the model without additional fitting (Fig. S4). The fitted parameters are shown in Table S2.

We define the goodness of the fit to the experimental data by a cost function which is the sum of all squared distances between data points and the analytical solution of the model. We draw the initial parameter values from a uniform distribution and use the Powell method of gradient descent to search for the minimum of the cost function (Press 2002). Parameter sets are rejected if the final values lie outside biologically realistic values (ranges given in Tab. S4). Note that different initial conditions lead to a diversity of parameter sets (Fig. S2), showing that the cost function is essentially flat close to its minima in parameter space. We furthermore included two terms in the cost function which assured that synaptic changes induced by single calcium transients are small ($\gamma_p, \gamma_d \sim 50$), and that synaptic changes are slow compared to the calcium dynamics ($\tau \gg 1$ sec).

To better compare fit results obtained from different experimental data sets, we chose to fix the potentiation and depression thresholds, θ_p and θ_d. That allowed us to project all results onto the same $C_{\rm pre}$-$C_{\rm post}$ plane (Fig. S2). Note that $\theta_p > \theta_d$ is consistent with (O'Connor et al. 2005) showing that blocking kinases reveals LTD for a protocol inducing LTP otherwise. Also, the unstable fix point, $\rho_\star$, and the fraction of synapses initially in the DOWN state, β, were fixed. Allowing θ_p, θ_d, $\rho_\star$ and β to be optimized by the fit routine did not considerably improve the match with experimental data. All other parameters are free parameters optimized during the fit (see Tab. S2).

References

Bear, M. F., L. N. Cooper, and F. F. Ebner (1987, Jul). A physiological basis for a theory of synapse modification. *Science 237*(4810), 42–48.

Bi, G. and M. Poo (1998, Dec). Synaptic modifications in cultured hippocampal neu-

rons: dependence on spike timing, synaptic strength, and postsynaptic cell type. *J Neurosci 18*(24), 10464–72.

Bienenstock, E. L., L. N. Cooper, and P. W. Munro (1982, Jan). Theory for the development of neuron selectivity: orientation specificity and binocular interaction in visual cortex. *J Neurosci 2*(1), 32–48.

Cormier, R. J., A. C. Greenwood, and J. A. Connor (2001, Jan). Bidirectional synaptic plasticity correlated with the magnitude of dendritic calcium transients above a threshold. *J Neurophysiol 85*(1), 399–406.

Gilbert, E. N. and H. O. Pollak (1960). Amplitude distribution of shot noise. *Bell Syst Tech J 39*, 333–350.

Hansel, C., A. Artola, and W. Singer (1997, Nov). Relation between dendritic ca2+ levels and the polarity of synaptic long-term modifications in rat visual cortex neurons. *Eur J Neurosci 9*(11), 2309–2322.

Nevian, T. and B. Sakmann (2006, Oct). Spine Ca2+ signaling in spike-timing-dependent plasticity. *J Neurosci 26*(43), 11001–11013.

O'Connor, D. H., G. M. Wittenberg, and S. S.-H. Wang (2005, Aug). Dissection of bidirectional synaptic plasticity into saturable unidirectional processes. *J Neurophysiol 94*(2), 1565–73.

Press, W. (2002). *Numerical Recipes in C++*. Cambridge University Press.

Risken, H. (1996). *The Fokker-Planck equation*. Springer.

Sabatini, B. L., T. G. Oertner, and K. Svoboda (2002, Jan). The life cycle of Ca(2+) ions in dendritic spines. *Neuron 33*(3), 439–52.

Sjöström, P., G. Turrigiano, and S. Nelson (2001, Dec). Rate, timing, and cooperativity jointly determine cortical synaptic plasticity. *Neuron 32*(6), 1149–64.

Wang, H.-X., R. C. Gerkin, D. W. Nauen, and G.-Q. Bi (2005, Feb). Coactivation and timing-dependent integration of synaptic potentiation and depression. *Nat Neurosci 8*(2), 187–93.

Wittenberg, G. M. and S. S.-H. Wang (2006, Jun). Malleability of spike-timing-dependent plasticity at the CA3-CA1 synapse. *J Neurosci 26*(24), 6610–6617.

Yang, S., Y. Tang, and R. Zucker (1999, Feb). Selective induction of LTP and LTD by postsynaptic [Ca2+]i elevation. *J Neurophysiol 81*(2), 781–7.